JCTC Journal of Chemical Theory and Computation

Bonding in Classical and Nonclassical Transition Metal Carbonyls: The Interacting Quantum Atoms Perspective

Davide Tiana,[†,⊥] E. Francisco,[‡] M. A. Blanco,[‡] P. Macchi,[§] Angelo Sironi,[†] and A. Martín Pendás*[,‡]

Department of Structural Chemistry and Inorganic Stereochemistry, University of Milan, Via Venezian 21, 20133 Milan, Italy, Departamento de Química Física y Analítica, Facultad de Química, Universidad de Oviedo, 33006-Oviedo, Spain, and Department of Chemistry and Biochemistry, University of Bern, Switzerland

Received December 9, 2009

Abstract: Chemical bonding in simple transition metal carbonyls is examined under the interacting quantum atoms approach (IQA), which provides an energetic viewpoint within the quantum theory of atoms in molecules (QTAIM). We have studied both classical and nonclassical isoelectronic series of complexes, with different coordinations and geometries and studied the evolution of the IQA interatomic interactions, using several levels of theory. Our results in classical carbonyls are compatible with the standard Dewar−Chatt−Duncanson model, although multicenter bonding may have an important role in some complexes. The increase (decrease) in the CO distance upon bonding is faithfully coupled to a decrease (increase) in the CO covalent energy, although the main energetic change in the CO moiety is electrostatic and due to charge transfer and/or polarization of its electron density. The metal−ligand interaction energy is dominated by covalent effects and depends strongly on the total net charge of the complex, being larger for negatively charged molecules, where π-back-donation is very important. The electrostatic (ionic-like) metal−ligand interaction energy is small in general, although it becomes more and more stabilizing with increasing coordination number.

1. Introduction

The metal (M) carbonyl (CO) interaction has probably sparked more interest than any other in metallorganic chemistry. This importance stems from its paradigmatic role in chemical bonding theory as well as in surface chemistry and catalysis.

As bonding is regarded, the M−CO interaction is generally gauged against the classical model proposed by Dewar, Chatt, and Duncanson (DCD) in 1951.[1,2] Succintly, a synergistic interaction is proposed to occur between σ charge donation from the CO highest occupied molecular orbital (HOMO) and a consequent π-back-donation from the M d orbitals to the CO lowest unoccupied molecular orbital (LUMO). Since its proposal, most theoretical works, using very many interpretation tools that range from Kitaura−Morokuma energetic decompositions to Natural Bond Orbital (NBO) analyses or real space techniques like those based on the Quantum Theory of Atoms in Molecules (QTAIM) or the use of the Electron Localization Function (ELF), have corroborated the essence of the DCD model.[3−8]

It is generally thought, for instance, that although the σ donation is larger than the π-back-donation, their energetic bonding role is reversed,[9] and the back-donation contribution is actually dominant.[10,11] From a simple molecular orbital (MO) perspective, the CO HOMO is its 5σ orbital, while the LUMO is a relatively low lying $2\pi^*$ function. Similarly, the metal frontier orbitals are the (crystal field splitted) d orbitals. The success of the DCD model is based on its simple, straightforward qualitative predictions. For instance,

* Corresponding author e-mail: angel@fluor.quimica.uniovi.es.
[†] University of Milan.
[‡] Universidad de Oviedo.
[§] University of Bern.
[⊥] Previous address: Departamento de Química Física y Analítica, Facultad de Química, Universidad de Oviedo, 33006-Oviedo, Spain.

10.1021/ct9006629
Published on Web 03/19/2010

it has been repeatedly reported that, for the CO bond, the 5σ orbital is either nonbonding,[12] or slighty antibonding,[13] while the nature of the $2\pi^*$ is definitely antibonding. In this way, the flow of electrons into the latter easily rationalizes the weakening of the CO bond, with its consequent lengthening[14] and reduction of stretching frequencies.[15] These two effects are standardly used to quantify the back-donation and evaluate the (reduced) CO bond strength.

A number of other experimental facts stem from similar DCD MO arguments. Back-bonding, for instance, clearly depends on the d$-2\pi^*$ energy gap,[16] which in turn is related to the electron−nuclear attraction and then, for an isoelectronic series, to the M atomic number. Since π-back-bonding implies a withdrawal of electronic density from M to the CO ligand, it is related to the M ionization potential. Further, π-back-donation being a shorter ranged interaction than σ donation, it turns out to be relatively sensible to the M covalent radius. Thus, relativistic effects and lanthanide contractions play a non-negligible role in its magnitude.[17]

The model illustrated so far was first questioned in the 1970s when, for the first time, the metal carbonyl cations $Cu(CO)_n^+$, $n = 1$ and 2, were synthesized.[18] These examples were followed by other homoleptic noble metal carbonyls like $Ag(CO)_n^+$, $n = 1$ and 2, or $Au(CO)_2^+$. Their common feature was a higher CO stretching frequency than that found in free CO (2143 cm^{-1}), so they were called "nonclassical" by Strauss et al.[17] The effect was ascribed to the absence of π-back-donation, such that the remaining weak σ donation removed density from the antibonding 5σ orbital, this resulting in a shorter CO bond with a larger force constant. Criticisms about the arbitrariness of such an explanation soon arrived,[19,20] and for instance, the antibonding character of the 5σ MO was put into question. Not only did a few studies demonstrate that this orbital was not antibonding, but also that the CO bond stiffenning was correctly reproduced by just modeling the electric field induced by the M cation. Slowly, an image in which the density redistribution induced by this field increased the covalency of the CO bond emerged.[21,22]

It is now relatively clear that it is not so easy to correlate CO stretching frequencies or force constants to M−CO back-donation due to mode coupling, that Strauss' inverse correlation between M−C and C−O distances may fail,[21] and that back-bonding is basically dependent on the M−CO distance, so that a particular onset distance exists for nearly every system that may be larger or smaller than its particular equilibrium geometry.[23] It has even been shown that the amount of donation−back-donation cannot be used as an indicator of binding energies.[24]

Real space analyses of chemical bonding in transition metal carbonyls have also been commonplace, in both the QTAIM and ELF flavors.[20,23,7,5,6] The MC bond is usually characterized by large positive laplacians at the bond critical point (bcp), with relatively large delocalization indices (δ^{AB}) for the MC pair. According to the QTAIM indicators, the MC bond has characteristics similar to those found in dative interactions of main group elements. Attempts to validate the DCD model have also been made either by partitioning densities into σ and π contributions,[7] by showing how the δ^{MO} correlates, as expected, with back-bonding,[5,25] or by using the domain averaged Fermi hole (DAFH) technique,[26] as introduced by Ponec.[27,28] The DCD model has also been examined in terms of real space valence charge concentrations for the metal−olefin link.[29] The solid theoretical foundation of these real space techniques is making them increasingly popular in the field of chemical bonding in transition metal (TM) chemistry.[8] However, a real space energetic image of these important bonds is lacking, and our interacting quantum atoms approach (IQA) may clearly fill this gap.

IQA[30−34] provides a theory of cohesion within the QTAIM by extending the domain partitioning of one-electron observables to interelectron repulsions. By doing so, we get an exact, chemically appealing partition of the molecular energy that may be recast into an easy to comprehend language. Within IQA, binding is the result of a competition between atomic deformation, which is an analogue of the classical promotion energy needed for an atom to get bonded to another, and pairwise additive interatomic interaction energies. The latter are made up of classical (or ionic-like) and exchange-correlation, purely quantum mechanical (or covalent-like) components. IQA has now been applied to provide a real space energetic view of a wide number of problems,[35−37] to shed some light into core concepts of the QTAIM,[38] and to propose statistical images of the chemical bond.[39−42] Recently, we have shown how to generalize its framework to wave functions containing effective core potentials (ECPs),[43] opening a window to examine chemical bonding issues in TM chemistry.

In this paper, we will examine the energetics of simple metal carbonyls under the IQA light, paying particular attention to the possible difference between classical and nonclassical systems. We will also show how many of the accepted energy features of the DCD model are translated into state of the art, orbital invariant real space analyses.

The layout of the paper is as follows. First, a brief summary of the IQA procedure will be presented, followed by a description of the computational details of our calculations. Then, we will describe our results in a number of classical and nonclassical carbonyls. We will end with some conclusions.

2. Brief IQA Survey and Summary

Let us succintly introduce a survey of the IQA parlance. Full accounts may be found elsewhere.[30−34] Let us start with a QTAIM partition of the space into atomic domains.[44] Then, at any molecular geometry,

$$\begin{aligned} E = & \sum_A (T^A + V_{en}^{AA} + V_{ee}^{AA}) \\ & + \sum_{A>B} (V_{nn}^{AB} + V_{en}^{AB} + V_{ne}^{AB} + V_{ee}^{AB}) \\ = & \sum_A E_{self}^A + \sum_{A>B} E_{int}^{AB} \end{aligned} \quad (1)$$

where $A \equiv \Omega_A$ is the atomic basin of nucleus A; T^A is its atomic kinetic energy; and V_{en}, V_{ne}, V_{ee}, and V_{nn} are the potential energies describing the several pair interactions

between the electrons and nuclei that reside in basins A and B, in an easy to decode terminology. Now, IQA uses ideas borrowed from McWeeny's[45] electronic separability to gather the above terms using chemical insight. All intrabasin terms are added to define the self-energy of a quantum atom (or group) E^A_{self}, while the interbasin ones are gathered in the interaction energy between pairs of atoms, E^{AB}_{int}. This interaction energy may be further partitioned into a classical component, V^{AB}_{cl}, obtained by adding V_{en}, V_{ne}, and V_{nn}; the Coulombic part of V_{ee}, V^{AB}_{C}; and a quantum mechanical, nonclassical, or exchange correlation term $V^{AB}_{xc} = V^{AB}_{ee} - V^{AB}_{C}$. This may always be done, so $E^{AB}_{int} = V^{AB}_{cl} + V^{AB}_{xc}$. When particular energetic references exist for the quantum groups, $E^{A,0}_{self}$, we define atomic deformation energies, $E^A_{def} = E^A_{self} - E^{A,0}_{self}$, such that molecular binding is the result of a competition between terms with the same order of magnitude: group deformation (which is usually positive) and intergroup interaction (overall negative):

$$E_{bind} = \sum_A E^A_{def} + \sum_{A>B} (V^{AB}_{cl} + V^{AB}_{xc}) \quad (2)$$

We have shown[32,34] that the classical and exchange-correlation interaction components are associated with the conventional notions of ionicity and covalency, so IQA translates quantum-mechanical energetic quantities into standard chemical concepts.

The formalism is immediately extended if several quantum groups are gathered to form functional groups $\mathscr{G}$, $\mathscr{H}$, etc.[32,34] Equation 1 applies for groups, too, if $E^{\mathscr{G}}_{self}$ is defined to contain all intragroup energetic components, and also eq 2 if whole-group references are used to define $E^{\mathscr{G}}_{def}$. In this work, it will be useful to consider each carbonyl ligand (L) as a quantum group, such that $\Omega_L = \Omega_C \cup \Omega_O$. In this way, we may discuss either the ML link interaction as a whole or each of its MC and MO components. Also, it is advantageous to discuss the changes in the ligand-related properties with respect to those in the isolated CO molecule, introducing the notation $\Delta X = X$ (coordinated L) $- X$ (free L). Using this notation, with free CO as a reference, the ligand deformation energy can be written as $E^L_{def} = \Delta E^C_{self} + \Delta E^O_{self} + \Delta E^{CO}_{int}$. Binding of the n CO ligands to the metal will thus comprise n ML interactions, $E^{ML}_{int} = E^{MC}_{int} + E^{MO}_{int}$, n of the above-mentioned ligand deformation energies measuring the cost in coming from the free CO state into the complex, plus the much smaller LL interactions, and the metal deformation energy E^M_{def}.

3. Computational Details

IQA partitioning, necessarily based on numerical integration techniques, is computationally intensive[30] and requires well-defined first and second order density matrices. Thus, only Hartree−Fock (HF) or variational multiconfigurational techniques may be used. Since the literature on M−CO systems is huge, much is known about the performance and limitations of methods with different levels of approximation for the treatment of electron correlation. For instance, Sherwood and Hall[46] showed that 97% the total energy is recovered at the HF level for $Cr(CO)_6$. At this moment, it is well-known that MP2 results paralell those trends found at the SCF level, with only quantitative differences. Single determinant approaches give rise to lower binding energies, thus longer MC and shorter CO distances,[47] and to underestimated π-back-donating but reasonable σ-donating effects.[24]

Less is known about the performance of DFT techniques as chemical bonding is regarded in these compounds. The B3LYP functional seems to overestimate back-donation,[8] which has turned out to be quite sensitive to the exchange-correlation functional.[21] Similarly, both BLYP and B3LYP overestimate binding energies giving rise to long MC distances in $CuCO^+$ and $CuCO^{2+}$.[48] All in all, whenever a multiconfigurational calculation cannot be undertaken due to computational constraints, a simple HF wave function provides a reasonable account of the major binding forces acting on simple transition metal carbonyls. Thus, we present here a combination of HF, CASSCF, and DFT (approximate) results.

All electronic structure calculations were performed with GAMESS.[49] H and main group elements were modeled with a 6-31G(d,p) basis set, while standard Hay and Wadt small core relativistic ECPs together with their standard basis sets (3s4s1s3p1p1p4d1d) were used for the transition metals.[50] IQA analyses were done with our PROMOLDEN code, and ECPs were treated according to our previously published protocol,[43] with M core densities obtained from 3-21G basis sets added in the computation of appropriate interatomic surfaces. It is important to recall that deformation energies are not accessible with our protocol for those quantum atoms bearing ECPs.[43] In the present case, we thus have access to E^L_{def}, but not to E^M_{def}, so we will only briefly consider the ligand deformation energies in a subset of our calculations, focusing the discussion on the ML interactions.

We have studied several ideal low-spin isoelectronic series at the HF level: The d^{10} T_d $[Fe(CO)_4]^{2-}$, $[Co(CO)_4]^-$, $Ni(CO)_4$, $[Cu(CO)_4]^+$, and $Pd(CO)_4$ systems, together with their d^8 D_{4h} $[Ni(CO)_4]^{2+}$ and $[Pd(CO)_4]^{2+}$ planar counterparts; the d^8 D_{3h} $[Mn(CO)_5]^-$, $Fe(CO)_5$, $[Co(CO)_5]^+$, and $Ru(CO)_5$ pentacarbonyls; and the d^6 O_h $[Ti(CO)_6]^{2-}$, $[V(CO)_6]^-$, $Cr(CO)_6$, $[Mn(CO)_6]^+$, and $[Fe(CO)_6]^{2+}$ species. Homoleptic noble metal cations $[M(CO)_n]^+$, M = (Cu, Ag, Au) with n = 1 and 2, have also been studied at the CASSCF//MP2 level with an active space comprising the five valence M d orbitals supplemented with the five outer orbitals of each carbonyl and four suitable low-lying virtuals. Due to the lack of appropriate basis sets, no core density was added in the CASSCF calculations. In order to test how IQA performs when using a Kohn−Sham determinant to approximately construct first- and second-order density matrices, we also performed some test DFT calculations at MP2 geometries for $[Ag(CO)_2]^+$ and $[Au(CO)_2]^+$. Several functionals have been used: BLYP; BLYP-LC; and the M06-l, M06, and M06-HF series, characterized by 0%, 27%, and 100% HF exchange, respectively. The d^{10} T_d molecules were also computed at the M06 level. To ascertain the role of electrostatic effects in nonclassical carbonyls, we have also computed the HCO^+ and COH^+ systems at the equivalent CASSCF level. Wave functions for the isolated CO ligand

Table 1. Basic Geometric and QTAIM Integrated Properties Together with IQA Interactions for the $[Fe(CO)_4]^{2-}$, $[Co(CO)_4]^{-}$, $Ni(CO)_4$, $[Cu(CO)_4]^{+}$, and $Pd(CO)_4$ d^{10} T_d Tetracarbonyls[a]

M	Fe	Co	Ni	Cu	Pd
d(MC)	1.735	1.766	1.924	2.296	2.229
Δd(CO)	0.049	0.024	0.002	−0.010	0.000
$\Delta\nu$	−491	−295	−64	90	−32
Q^M	0.282	0.189	0.122	0.802	0.064
Q^L	−0.570	−0.297	−0.031	0.050	−0.016
ΔQ^C	−0.439	−0.234	−0.086	−0.035	−0.025
δ^{MC}	1.347	1.153	0.798	0.313	0.623
δ^{MO}	0.198	0.166	0.097	0.024	0.075
δ^{CC}	0.130	0.084	0.039	0.012	0.016
$\Delta\delta^{CO}$	−0.318	−0.231	−0.046	0.037	−0.056
E_{int}^{ML}	−0.343	−0.277	−0.192	−0.070	−0.131
E_{int}^{MC}	−0.215	−0.187	−0.142	0.122	−0.098
ΔE_{int}^{CO}	0.374	0.220	0.212	0.050	0.044
V_{cl}^{ML}	−0.008	0.011	0.005	−0.005	0.002
V_{cl}^{MC}	0.100	0.084	0.045	0.185	0.029
ΔV_{cl}^{CO}	0.312	0.180	0.224	0.068	0.040
V_{xc}^{ML}	−0.334	−0.288	−0.197	−0.067	−0.134
V_{xc}^{MC}	−0.314	−0.271	−0.187	−0.065	−0.127
ΔV_{xc}^{CO}	0.063	0.041	−0.011	−0.017	0.004
E_{def}^{L}	0.236	0.179	0.110	0.064	0.087

[a] HF data in atomic units, except distances in Å and frequencies in cm^{-1}. Parameters for the isolated CO molecule are as follows: d(CO) = 1.114, ν(CO) = 2439, Q^C = 1.403, δ^{CO} = 1.508, E_{int}^{CO} = −2.120, V_{cl}^{CO} = −1.706, and V_{xc}^{CO} = −0.415. Recall that $\Delta X = X$ (coordinated L) − X (free L).

have been obtained for comparison purposes at all the computational levels previously described.

PROMOLDEN integrations have been performed using typically tight parameters, truncated at $l_{max} = 10$, with 631-point radial and 5810-point Lebedev angular grids. β-spheres up to $l = 6$ with radii equal to 90% of the distance from the nuclear position to the closest bcp have been used, and 431 radial and 534 Lebedev angular grid points have been selected for them. These are fairly standard computational conditions for IQA calculations[32] that usally provide interactions converged to about 1 kcal/mol.

Since IQA interaction energies vary in wide ranges, we will use atomic units for them in all of our tables. However, some of the arguments in the text will refer to relevant differences among them. In those cases, we will shift to kilocalories per mole to provide more chemically meaningful quantities.

4. Bonding in the T_d $M(CO)_4$ Systems

Let us examine the isoelectronic d^{10} T_d Fe, Co, Ni, Cu, and Pd tetracarbonyls from our IQA perspective. We will start with a brief analysis of some standard QTAIM integrated quantities. Table 1 contains topological charges, Q, and delocalization indices, δ, for our systems, including the isolated CO ligand.

Although these kind of results are known, it should be noticed that all the metals bear small positive topological charges, meaning that, in the most simple DCD model, back-bonding should be extremely large in the Fe compound, for instance. The geometric correlations of the model, as briefly explained in the Introduction, do also come out easily from the computed data. For instance, the changes in the CO stretching frequencies upon bonding, the changes in d (CO), and the total net charge of the ligand correlate among each other. Notice that the total charge of the ligand is mostly absorbed by the C atom, so charge transfer is fairly localized in the MC region.

Similar insight is obtained from electron delocalization properties, like the delocalization index, δ, a measure of bond order in real space. For 3d metals, the MC bond order decreases as the MC distance increases, as expected. In line with DCD, this increase is coupled to a lengthening of the CO distance and a decrease in the CO bond order. Not so obviously, however, it is also clear that δ^{CO} does also correlate with the overall CO (L) polarization. The only system in which the L net charge is positive is $[Cu(CO)_4]^{+}$, meaning that charge transfer goes from the ligand to the metal in a σ-like fashion. This is also a possible nonclassical carbonyl, with smaller d(CO) and larger δ^{CO} than those found in free CO. Polarization of the CO ligand as induced by the metal is clearly related to the CO bond covalency, as pointed out by Lupinetti and co-workers.[23] Finally, another interesting point is related to the non-negligible δ^{CC} value that exists between adjacent L's in the Co and Fe compounds. This points toward an important multicenter character of the M−L bonding in those cases where back-bonding is also deemed important, i.e., in electron-rich compounds. As we will show with our DAFH analyses, this is true and should be understood as one limitation of the DCD view.

The energetic view provided by IQA enlightens the above comments. Let us start with a fine-grained view, by examining the MC and MO IQA quantities. E_{int}^{MC} is large and splits the T_d systems into two categories of negative and positive total MC interaction. As we will see, this is related to the total Q^L charge, and positive MC total interactions will become common for other stoichiometries. The V_{cl}^{MC} contribution to the MC interaction is destabilizing, due basically to the positive net charge at the metal site. However, its particular value is the result of a complex balance among the MC distance, the positive net M and C charges, and the polarization of the charge distribution. The covalent contribution to the MC bond, provided by V_{xc}^{MC}, follows the total net charge of the complex. Its value in the Fe, Co, and Ni compounds, about −200 kcal/mol in the first, is considerably large if we compare it to the −260 kcal/mol value obtained for the free CO ligand, V_{xc}^{CO}, a formal triple bond. MC covalency is the basic stabilizing interaction in this series, and even in the Cu case, where back-bonding is thought to have a minor role, it amounts to about −40 kcal/mol. The MO interactions may be obtained from the table by subtraction (MO = ML − MC) and deserve similar comments. E_{int}^{MO} is obviously stabilizing, controlled by the negative electrostatic component which may be faithfully approximated by a point charge contribution, and its range of variation is smaller. Just as delocalization between the metal and the oxygen atom of each carbonyl provides a real space measure[25] of the relative intensity of π-back-donation, V_{xc}^{MO} gives us its energetic signature. It is negligible in $[Cu(CO)_4]^{+}$, about 1 kcal/mol, and 10 times larger in the $[Fe(CO)_4]^{2-}$ anion. Notice that V_{xc}^{MO} is always smaller than 7% V_{xc}^{MC}: this property should not be interpreted as a direct measure of the total energetics associated with back-donation, which

does also include the C atom of the ligand, but rather as an isolated energetic signature, not affected by the covalent contribution of σ donation.

Moving to group interactions, the total $E_{int}^{ML} = E_{int}^{MC} + E_{int}^{MO}$ is always negative, although in the Cu case it is relatively small, −44 kcal/mol. Notice that its classical component is small, its absolute value not exceeding 7 kcal/mol, and that it oscillates from positive to negative. Thus, even if each of the MC and MO electrostatic terms may be large, the polarization pattern of L conspires to overall small V_{cl}^{ML} values such that in the end it is covalency, not electrostatics, that governs the ML bonding. Continuing with the group description of the CO ligands, their energetic change upon bonding deserves comment. The overall CO deformation energy, E_{def}^{L}, is positive (as found in most of the systems examined by IQA up to now) and is clearly correlated to the total net charge of the ligand, Q^{L}. This is expected, since, in the case of highly heteropolar links, self-energies are controlled by ionization costs. Notice that the deformation energy in the Cu complex, with a rather low positive net charge, is relatively small, about 40 kcal/mol. In all the cases examined, deformation of the ligand is dominated by ΔE_{int}^{CO}; we will concentrate on its components and will not consider E_{def}^{L}'s themselves again.

Regarding the different properties involved in the CO deformation upon coordination, Δd^{CO}, $\Delta\delta^{CO}$, and ΔV_{xc}^{CO} are quite linearly correlated, whereas ΔV_{cl}^{CO} is not. In agreement with previous IQA knowledge, and also with the results by Lupinetti and co-workers,[23] the CO distance responds basically to changes in covalency. These coordinated CO bonds display V_{xc}^{CO} values smaller than those in free CO (except in the Cu complex), so ML bonding decreases the covalency of the CO bond. Although V_{cl}^{CO} shows a relatively complex pattern, the simple $Q^{C}Q^{O}/d^{CO}$ point charge term correlates rather well with it. In general, depolarization of a bond leads to a decrease in its electrostatic contribution, as may be rationalized from the smaller value of $(q - \varepsilon)(-q + \varepsilon)$ with respect to $-q^2$ in Coulomb's law when charge is transferred from one point charge to the other in an ionic pair.

We also note that, although in the Cu compound the covalent CO interaction energy is comparable but smaller than that in the free CO molecule, its electrostatic interaction is considerably (by about 60 kcal/mol) larger. The combination of both facts justifies its d (CO), 0.01 Å smaller than the free value. We want to stress that Δd (CO), Q^{L}, $\Delta\delta^{CO}$, E_{int}^{MC}, and ΔV_{xc}^{CO} all change sign in this complex with respect to the rest of the series, so the overall positive charge of the species has a big impact on its detailed energetics.

The behavior of the neutral Pd complex is also noteworthy, at least when compared to the also neutral Ni case. This is probably related to its large ionization potential that justifies its smaller Q^{M} and the relatively small change in the net charges that it induces on the CO ligand. However, the effect of its diffuse d shell on the ligand is not small, and the CO moiety suffers a rather big density polarization that increases its classical attraction.

Table 2 summarizes our M06 DFT results in the same set of complexes. We must stress that standard Kohn−Sham (KS) DFT calculations lack a properly defined second order density matrix, so our V_{xc} and δ values are approximate, obtained by constructing a Dirac−Fock pseudo-pair density from the KS determinant. There is nevertheless evidence[51] that DFT δ's do compare reasonably well with wave function based values.

Table 2. DFT M06 Geometric and QTAIM Integrated Properties for the T_d Complexes[a]

M	Fe	Co	Ni	Cu	Pd
d(MC)	1.745	1.764	1.843	2.038	2.081
Δd(CO)	0.055	0.029	0.006	−0.010	0.004
Q^{M}	0.327	0.119	0.305	0.684	0.250
Q^{L}	−0.582	−0.280	−0.077	0.079	−0.063
ΔQ^{C}	−0.480	−0.252	−0.128	−0.054	−0.110
δ^{MC}	1.404	1.259	0.968	0.565	0.874
δ^{MO}	0.240	0.213	0.148	0.059	0.132
δ^{CC}	0.141	0.103	0.067	0.034	0.038
$\Delta\delta^{CO}$	−0.333	−0.242	−0.113	0.032	−0.077
E_{int}^{ML}	−0.368	−0.329	−0.244	−0.126	−0.192
E_{int}^{MC}	−0.253	−0.272	−0.154	0.024	−0.116
ΔE_{int}^{CO}	0.441	0.302	0.206	0.149	0.177
V_{cl}^{ML}	−0.019	−0.004	0.002	0.009	0.007
V_{cl}^{MC}	0.073	0.032	0.078	0.153	0.071
ΔV_{cl}^{CO}	0.384	0.270	0.204	0.178	0.181
V_{xc}^{ML}	−0.350	−0.325	−0.246	−0.135	−0.199
V_{xc}^{MC}	−0.327	−0.304	−0.232	−0.129	−0.187
ΔV_{xc}^{CO}	0.057	0.033	0.002	−0.029	−0.004

[a] Data for the isolated CO species: d(CO) = 1.137, Q^{C} = 1.209, δ^{CO} = 1.726, E_{int}^{CO} = −1.773, V_{cl}^{CO} = −1.310, and V_{xc}^{CO} = −0.463. The structure of the table repeats that found in Table 1.

All of our previous arguments apply, mostly unchanged, to the DFT data. This fact seems to support the soundness of these IQA procedures based on Dirac−Fock density matrices constructed from KS determinants. A couple of points deserve mentioning, nevertheless. The DFT free CO molecule description takes into account, even with the above-mentioned approximations, the rather large change in polarization caused by electron correlation. This is seen in the clearly smaller DFT Q's and V_{cl}^{CO} interaction and in a noticeably larger V_{xc}^{CO}. Formation of the complexes gives rise to a decrease in the overall polarity of CO, and both the Q and V_{cl}^{CO} values decrease markedly. The DFT free or coordinated CO is clearly less ionic and more covalent than the HF one. As expected, correlation increases back-donation as measured by δ^{MO}. Notice how in the Cu compound V_{xc}^{CO} has now decreased below the free CO value by about 20 kcal/mol. This is consistent with the onset of a nonclassical carbonyl.

5. Classical Penta- and Hexacarbonyls

We will summarize in this section our results on the d^8 D_{3h} pentacoordinated and octahedral classical carbonyls. Tables 3 and 4 show that most of our comments regarding the $M(CO)_4$ species hold in these compounds.

The pentacarbonyls are characterized by well differentiated axial and equatorial ML bonds. It is well-known that the equatorial link is generally stronger and shorter, but this gets reversed in the Co case. In this latter complex, the overall topological charge of the CO ligands is positive, as in $[Cu(CO)_4]^+$. It is also known, though nonetheless interesting, that the metal is quite positively charged even in the Mn

Table 3. Geometric, QTAIM Integrated Properties, and IQA Interactions for the d^8 D_{3h} $[Mn(CO)_5]^-$, $Fe(CO)_5$, $[Co(CO)_5]^+$, and $Ru(CO)_5$ Complexes[a]

M	Mn	Fe	Co	Ru
$d(MC)_{ax}$	1.937	2.061	2.176	2.047
$d(MC)_{eq}$	1.822	1.875	2.251	2.043
$\Delta d(CO)_{ax}$	0.013	−0.002	−0.011	0.000
$\Delta d(CO)_{eq}$	0.030	0.008	−0.009	0.006
$\Delta\nu_{ax}$	−192	−11	140	−50
$\Delta\nu_{eq}$	−360	−188	0	−113
Q^M	0.678	0.570	0.852	0.515
Q^L_{ax}	−0.192	−0.034	0.036	−0.061
Q^L_{eq}	−0.431	−0.156	0.025	−0.139
ΔQ^C_{ax}	−0.155	−0.118	−0.051	−0.136
ΔQ^C_{eq}	−0.369	−0.232	−0.050	−0.209
δ^{MC}_{ax}	0.750	0.521	0.365	0.834
δ^{MC}_{eq}	1.100	0.933	0.377	0.955
δ^{MO}_{ax}	0.110	0.059	0.030	0.106
δ^{MO}_{eq}	0.158	0.123	0.032	0.126
δ^{CC}_{axeq}	0.105	0.069	0.038	0.055
$\Delta\delta^{CO}_{ax}$	−0.186	−0.028	0.012	−0.076
$\Delta\delta^{CO}_{eq}$	−0.234	−0.067	0.018	−0.055
E^{MLax}_{int}	−0.204	−0.130	−0.094	−0.203
E^{MLeq}_{int}	−0.318	−0.231	−0.087	−0.226
E^{MCax}_{int}	0.009	0.029	0.125	−0.042
E^{MCeq}_{int}	−0.095	−0.065	0.119	−0.078
ΔE^{COax}_{int}	0.153	0.214	0.069	0.226
ΔE^{COax}_{int}	0.309	0.344	0.059	0.317
V^{MLax}_{cl}	−0.024	−0.010	−0.012	−0.007
V^{MLeq}_{cl}	−0.048	−0.002	−0.006	−0.004
V^{MCax}_{cl}	0.178	0.143	0.204	0.144
V^{MCeq}_{cl}	0.159	0.151	0.197	0.132
ΔV^{COax}_{cl}	0.124	0.225	0.084	0.230
ΔV^{COeq}_{cl}	0.269	0.354	0.074	0.330
V^{MLax}_{xc}	−0.180	−0.120	−0.081	−0.195
V^{MLeq}_{xc}	−0.270	−0.227	−0.081	−0.222
V^{MCax}_{xc}	−0.169	−0.114	−0.078	−0.185
V^{MCeq}_{xc}	−0.254	−0.215	−0.078	−0.210
ΔV^{COax}_{xc}	0.031	−0.010	−0.014	0.003
ΔV^{COeq}_{xc}	0.041	−0.009	−0.014	−0.012

[a] HF data in atomic units, except distances in Å and frequencies in cm^{-1}.

Table 4. Geometric, QTAIM Integrated Properties, and IQA Interactions for the d^6 O_h $[Ti(CO)_6]^{2-}$, $[V(CO_6)]^-$, $Cr(CO)_6$, $[Mn(CO)_4]^+$, and $[Fe(CO)_6]^{2+}$ Systems[a]

M	Ti	V	Cr	Mn	Fe
d(MC)	2.036	1.986	2.012	2.159	2.225
Δd(CO)	0.041	0.023	0.005	−0.008	−0.016
$\Delta\nu$	−495	−288	−108	57	148
Q^M	1.461	1.188	0.930	0.994	1.153
Q^L	−0.574	−0.361	−0.154	0.002	0.141
ΔQ^C	−0.509	−0.352	−0.162	−0.071	−0.118
δ^{MC}	0.622	0.739	0.680	0.444	0.374
δ^{MO}	0.092	0.111	0.098	0.045	0.032
δ^{CC}	0.140	0.106	0.067	0.039	0.050
$\Delta\delta^{CO}$	−0.225	−0.175	−0.124	−0.012	0.156
E^{ML}_{int}	−0.324	−0.267	−0.192	−0.113	−0.090
E^{MC}_{int}	0.071	0.060	0.067	0.137	0.156
ΔE^{CO}_{int}	0.416	0.343	0.150	0.082	0.218
V^{ML}_{cl}	−0.187	−0.096	−0.034	−0.013	−0.004
V^{MC}_{cl}	0.200	0.221	0.216	0.232	0.239
ΔV^{CO}_{cl}	0.376	0.319	0.135	0.093	0.272
V^{ML}_{xc}	−0.138	−0.171	−0.158	−0.099	−0.085
V^{MC}_{xc}	−0.130	−0.161	−0.149	−0.095	−0.082
ΔV^{CO}_{xc}	0.041	0.025	0.015	−0.010	−0.053

[a] HF data in atomic units, except distances in Å and frequencies in cm^{-1}.

complex. This means that the ligands in the complexes bear a considerable negative charge, larger in the equatorial positions. The values of the average MC delocalization indices are similar to those found in the equivalently charged T_d molecules, and so is the covalent energy associated with the MC bond. There is however a tendency toward stronger (weaker) MC links for the negatively (positively) charged D_{3h} complexes when compared to their equivalently charged T_d counterparts. Together with δ^{MO}, our calculations show that π-back-bonding is largest in the Mn compound and smallest in the cobalt one. This also justifies the large positive metal charges. Our V_{xc} and V_{cl} values validate that, in general, the axial ML bonds are more ionic in the four D_{3h} cases than the equatorial ones, although in some cases the difference is small. A salient feature of our data is the positive value of these axial E^{MC}_{int}'s for all of the systems except $Ru(CO)_5$, so it is the very stabilizing MO interaction which stabilizes the ML link. This is related to the combined effect of the larger positive charges of the M and the axial carbon atoms. Contrarily to the uniform MC electrostatic behavior, there is a clear change in the MC covalency. The axial links in the Mn and Fe moieties are less covalent than the equatorial ones, while the opposite holds in the $Ru(CO)_5$ molecule.

As regards the CO moiety, it is relatively interesting to notice that the equatorial CO distance is larger than the axial one, independently of the M−C distance behavior. This correlates reasonably with delocalization indices and V_{xc} values, and as in the T_d compounds, $\Delta\delta$'s are considerably larger than ΔV_{xc}'s. In the Mn and Fe complexes, the axial carbonyls are slightly more covalent than the equatorial ones, but the situation is clearly reversed for $Ru(CO)_5$. As found in the tetrahedral cases, the total CO electrostatic interaction is related to the repolarization of the carbonyl group, increasing on average with $|\Delta Q^C|$. As with $[Cu(CO)_4]^+$, Δd(CO), Q^L, $\Delta\delta^{CO}$, E^{MC}_{int}, and ΔV^{CO}_{xc} change sign for $[Co(CO)]^+$. This consistency shows how intimately coupled the changes in the CO ligands are to the ML bonding features.

Finally, it is worthwhile noticing the similarity in the trends of the CO variations upon bonding for equally charged T_d and D_{3h} systems, e.g., $[Co(CO)_4]^-$ and $[Mn(CO)_5]^-$, and the prominent CC delocalizations in the Mn and Fe pentacarbonyls, which again point toward non-negligible multicenter bonding features among the carbonyls with covalent contributions as large as 10 kcal/mol.

Correlation effects may alter significantly the HF geometry of these compounds. For instance, the M06 geometry for $Fe(CO)_5$, one of the systems with more dramatic changes, gives axial and equatorial MC distances of 1.798 and 1.801 Å, respectively, with Δd(CO) equal to 0.010 and 0.012 Å in the same order. At this geometry, a HF IQA analysis provides $Q^M = 0.516$, so the total charge transfer has not changed much due to the geometry change, but other quantities depending on the quite shorter MC distances are altered as expected. For instance, $\delta^{MC}_{ax} = 0.829$ and $\delta^{MC}_{eq} = 0.994$. Similarly, $\delta^{MO}_{ax} = 0.106$ and $\delta^{MO}_{eq} = 0.129$. As the ML interactions are regarded, $V^{ML_{ax}}_{cl} = 0.005$ and $V^{ML_{eq}}_{cl} = 0.016$ au, while $V^{ML_{ax}}_{xc} = -0.209$ and $V^{ML_{ax}}_{xc} = -0.239$ au. The decrease in the ML distances thus leads to increased ML interactions, much more important in the axial than in the equatorial link.

The octahedral d^6 hexacarbonyls follow similar basic rules. As we move from Ti to Fe, the MC distance increases with the exception of the Ti molecule, and the CO bond length decreases monotonically, getting shorter than in the isolated molecule for both the Mn and Fe complexes, which also show positive Q^L values. Simultaneously, Q^M passes through

a minimum in the Cr complex. Notice how, as Q^L goes from negative to positive, ΔQ^C becomes decoupled from it. The double negative Ti anion has the largest positive metal charge and the most negatively charged CO species of all the examples examined up to now. However, both δ^{MC} and δ^{MO} and their V_{xc} covalent energy counterparts clearly show that back-bonding in these O_h complexes has saturated at the vanadium complex, and that in titanium the approach of the six carbonyls is only possible at a slightly larger MC final distance. This is accompanied by a quite large intercarbonyl delocalization, as measured by δ^{CC}. Another way to look at the same saturation stems from the metal localization index, $\lambda^{Ti} = 18.39$. This parameter grows monotonously up to 23.69 in the Fe hexacarbonyl. Only about 18 electrons (its [Ar] core) are localized in the Ti atomic basin as far as two-center delocalizations are regarded, so all of the valence has been used in bonding to a first approximation. This effect may explain the unexpectedly large TiC distance.

The O_h systems show very large M charges, thus positive total E_{int}^{MC} values independently of the value of Q^L. This behavior is different from that found in our previous example and makes the MO interaction decisive in accounting for the negative E_{int}^{ML} values and the stability of the complexes. We want to stress that, as we go from the tetra- to the hexacarbonyls, the value of E_{int}^{ML} turns out to be a function of the net charge of the complex and its coordination. For a given total charge of −2, −1, 0, +1, and +2, its most negative value, −0.34, −0.31, −0.23, −0.11, and −0.09 E_h, is attained for the $[Fe(CO)_4]^{-2}$, $[Mn(CO)_5]^-$, $Fe(CO)_5$, $[Mn(CO)_6]^+$, and $[Fe(CO)_6]^{2+}$ complexes, respectively. Thus, the ML interaction is most favorable for middle 3d metals, low coordinations, and negatively charged complexes. However, as the total charge becomes positive, higher coordinations become preferable (notice that we have only one dication in this series).

We also notice that the covalency of the MC interaction decreases on going from anions to cations (as back-bonding arguments suggest) for any coordination, except in $[Ti(CO)_6]^{2-}$, for which we have already suggested a saturation phenomenon. Moreover, the MC V_{xc} decreases with coordination, and as we move from tetra- to hexacarbonyls, the ML link becomes more ionic, as measured by V_{cl}^{ML}. This is a very well-known bonding tendency in solid state physics, where larger coordination phases tend to be more ionic and, in fact, a simple consequence of Pauling's rules. Overall, V_{cl}^{ML} is negligibile, except in penta- and hexacoordinated anions, where V_{xc}^{ML} peaks, so almost all of the ML stabilization energy comes from covalent contributions that may be small in cations.

With all the above arguments, the changes in the CO quantities of our $M(CO)_6$ molecules are easily rationalized. As seen in Table 4, both Δd (CO) and ΔV_{xc}^{CO} are negative in the Mn and Fe molecules. Their stronger CO links do also display a positive CO net charge with rather small negative Q^O and small δ^{MO}, thus very small back-bonding. As we will explore in the next section, both the change of sign and the decrease in magnitude of the CO polarity are signatures of this behavior.

Table 5. Geometric, QTAIM Integrated Properties, and IQA Interactions for the d^8 Square Planar $[Ni(CO)_4]^{2+}$ and $[Pd(CO)_4]^{2+}$ Complexes[a]

M	Ni	Pd		Ni	Pd
d(MC)	2.126	2.131	Q^M	1.490	1.104
Δd(CO)	−0.019	−0.020	Q^L	0.128	0.224
$\Delta\nu$	172	120	ΔQ^C	−0.057	0.035
δ^{MC}	0.383	0.614	E_{int}^{ML}	−0.091	−0.101
δ^{MO}	0.026	0.050	E_{int}^{MC}	0.264	0.171
$\Delta\delta^{CO}$	0.092	0.069	ΔE_{int}^{CO}	0.107	0.080
V_{cl}^{ML}	−0.004	0.042	V_{xc}^{ML}	−0.087	−0.143
V_{cl}^{MC}	0.348	0.309	V_{xc}^{MC}	−0.084	−0.138
ΔV_{cl}^{CO}	0.146	0.118	ΔV_{xc}^{CO}	−0.038	−0.036

[a] HF data in atomic units, except distances in Å and frequencies in cm^{-1}.

6. Nonclassical Carbonyls

Let us start by considering the d^8 square planar $[Ni(CO)_4]^{2+}$ and $[Pd(CO)_4]^{2+}$ 16-electron complexes. Table 5 summarizes our results. A first look confirms our previous observations: shortening instead of lengthening of d (CO), large metal positive topological charges, positive but small total net charge for the carbonyl ligands, relatively small MC delocalization indices coupled to very small δ^{MO} or back-bonding, and positive $\Delta\delta^{CO}$. Energetically, we find positive MC interaction energies with large negative E_{int}^{MO} and not too large covalent contributions that point to important MC ionicity, and as far as the CO ligand is regarded, larger covalency than in free CO. This provides an image in which almost all the characteristics of standard carbonyls have been reversed. Notice how, as we move from anionic to cationic species, the overall V_{cl}^{ML} passes from negative values to even destabilizing interactions, here exemplified by the $[Pd(CO)_4]^{2+}$ system. Its only overall stabilizing ML term is V_{xc}^{ML}, clearly dominated by the MC contribution.

Since there are a number nonclassical mono- and dicarbonyl cations traditionally considered as nonclassical, we have performed CASSCF calculations on some of them to ascertain the role of at least static correlation on the IQA energetic quantities of these complexes. Our results are gathered in Table 6.

Most of our previous findings apply unchanged. However, caution is necessary when comparing the CASSCF free CO quantities with those found in the complexes, since the limited amount of correlation accounted for does not affect the CO moiety in the same manner when isolated or interacting. Even with this in mind, we clearly see a shortening of the CO bond length in all the cases, positive CO net charges that increase with the coordination index, relatively small MC delocalization indices, and very low δ^{MO}'s, except in the gold complexes, which display a large covalency in the MC link and behave differently, see below. These systems do also show negative ΔV_{xc}^{CO} values and lowly polarized CO ligands with larger CO total interactions. In the dicarbonyls, ΔE_{int}^{CO} and even ΔV_{cl}^{CO} may become negative.

Notice that the total ML interaction energies are not small, peaking at −109 kcal/mol for the $Au(CO)^+$ molecule, and that the general behavior of the HCO^+ system parallels rather closely that of the gold compounds.

A comparison among the Cu, Ag, and Au compounds, on one hand, and of mono- and dicarbonyls, on the other, is

Table 6. HCO^+, Together with the d^{10} Linear $Cu(CO)^+$, $Ag(CO)^+$, $Au(CO)^+$, $[Cu(CO)_2]^+$, $[Ag(CO)_2]^+$, and $[Au(CO)_2]^+$ Data, in This Order, Calculated at the CASSCF Level with MP2 Geometries, as Described in the Text[a]

M	H	Cu	Ag	Au	Cu	Ag	Au
d(MC)	1.090	1.967	2.311	1.975	1.937	2.234	2.006
Δd(CO)	−0.015	−0.007	−0.006	−0.006	−0.006	−0.005	−0.007
$\Delta\nu$	13	95	77	90	107	120	119
Q^M	0.414	0.887	0.889	0.782	0.786	0.768	0.645
Q^L	0.586	0.114	0.111	0.220	0.108	0.118	0.179
ΔQ^C	0.281	−0.033	−0.011	0.043	0.030	0.113	0.151
δ^{MC}	0.687	0.567	0.434	0.975	0.573	0.483	0.855
δ^{MO}	0.058	0.036	0.026	0.080	0.039	0.032	0.072
$\Delta\delta^{CO}$	0.007	0.046	0.052	−0.031	0.109	0.144	0.123
E_{int}^{ML}	−0.090	−0.115	−0.079	−0.173	−0.121	−0.088	−0.166
E_{int}^{MC}	0.034	0.077	0.093	0.004	0.069	0.087	0.015
ΔE_{int}^{CO}	0.115	0.102	0.071	0.119	−0.004	−0.107	−0.099
V_{cl}^{ML}	0.129	0.014	0.011	0.057	0.014	0.016	0.043
V_{cl}^{MC}	0.247	0.202	0.180	0.226	0.200	0.188	0.216
ΔV_{cl}^{CO}	0.146	0.118	0.086	0.132	0.011	−0.092	−0.084
V_{xc}^{ML}	−0.220	−0.129	−0.090	−0.231	−0.135	−0.104	−0.209
V_{xc}^{MC}	−0.213	−0.125	−0.087	−0.223	−0.131	−0.101	−0.201
ΔV_{xc}^{CO}	−0.031	−0.016	−0.015	−0.013	−0.015	−0.015	−0.014

[a] All data in atomic units, except distances in Å and frequencies in cm^{-1}. CASSCF//MP2 data for isolated CO: d(CO) = 1.147, Q^C = 1.188, $\nu(CO)$ = 2137 cm^{-1}, δ^{CO} = 1.384, E_{int}^{CO} = −1.711, V_{cl}^{CO} = −1.295, and V_{xc}^{CO} = −0.416.

interesting by itself. Our data provide a fresh new perspective to some reported observations. For instance, it has been found[23] that the Cu and Ag dicarbonyls display larger electron and energy densities at the MC bond critical point than those in the monocarbonyls, but that the contrary is true for the Au compounds. This is interpreted in terms of larger/smaller covalent contributions using the empirical correlation between these quantities. Our V_{xc}^{MC} and V_{xc}^{ML} values provide direct support to these claims, being larger in the dicarbonyls except for the Au systems. There is also consensus about significant back-donation in $Au(CO)^+$, small back-donation in $Cu(CO)^+$, and negligible back-donation in $Ag(CO)^+$. Our δ^{MO} and V_{xc}^{MO} support this statement.

However, a rather constant argument in the literature ascribes a mainly electrostatic character to the ML link in $Ag(CO)^+$, for instance. Our analysis allows us to pinpoint the nature of this claim by using either the atomic or functional group point of view for the CO ligand. The overall AgC interaction energy is positive, thus destabilizing, by 58 kcal/mol, a result coming from a large electrostatic repulsion associated with 113 kcal/mol and a significant covalent interaction of −55 kcal/mol. It is only in this sense that the AgC link is mainly ionic in nature: it is the MO electrostatic attraction associated with an energy of −106 kcal/mol (and a weak covalent term of −2 kcal/mol) which leads to the overall negative AgL interaction of −50 kcal/mol. Shifting to the functional group view of the carbonyl ligand, as is usually done, the picture changes dramatically, for the overall V_{cl}^{ML} is now very small, +7 kcal/mol, and it is not electrostatics, but covalency, which binds the system.

The nature of the stiffening of the CO interaction in nonclassical carbonyls may also be explored with our procedure. We have thus performed equivalent CASSCF calculations to those presented in Table 6 in the HCO^+ and COH^+ systems for several HC or OH distances and relaxed CO bond lengths. Table 7 gathers the most interesting results.

Table 7. Topological Charges, Sharing Indices, and IQA Properties for the CASSCF Descriptions of HCO^+ and COH^+ as the HC or OH Distances (d) Are Varied with Respect to Their Respective Equilibrium Values: $\Delta d = d - d_{eq}$[a]

				HCO^+		
Δd	−0.2	−0.1	0.0	0.1	0.2	0.3
Δd(CO)	−0.002	−0.001	0.000	0.004	0.005	0.005
Q^L	0.699	0.574	0.521	0.554	0.529	0.511
ΔQ^C	0.418	0.302	0.257	0.268	0.248	0.234
Q^H	−0.301	0.426	0.477	0.443	0.469	0.488
δ^{HC}	0.884	0.791	0.744	0.650	0.615	0.584
$\Delta\delta^{CO}$	0.042	0.054	0.059	0.011	0.010	0.010
ΔE_{int}^{CO}	0.048	0.068	0.067	0.086	0.082	0.079
ΔV_{cl}^{CO}	0.083	0.104	0.103	0.121	0.116	0.112
ΔV_{xc}^{CO}	−0.035	−0.036	−0.036	−0.035	−0.034	−0.033
				COH^+		
Δd(CO)	−0.001	0.000	0.000	0.000	0.000	0.001
Q^L	0.410	0.324	0.270	0.232	0.202	0.190
ΔQ^C	0.274	0.263	0.252	0.242	0.231	0.220
Q^H	0.590	0.675	0.730	0.770	0.800	0.811
δ^{HO}	0.595	0.484	0.403	0.343	0.297	0.276
$\Delta\delta^{CO}$	−0.255	−0.269	−0.218	−0.200	−0.182	−0.168
ΔE_{int}^{CO}	0.104	0.079	0.067	0.062	0.059	0.061
ΔV_{cl}^{CO}	0.022	0.000	−0.008	−0.009	−0.008	−0.002
ΔV_{xc}^{CO}	0.083	0.079	0.075	0.071	0.067	0.063

[a] CO distances for the optimum HCO^+ and COH^+ molecules are 1.119 and 1.166 Å and should be compared to the isolated CASSCF CO one, 1.150 Å. All data in atomic units, except distances in Å.

First, the effect of the electric field imposed by the H proton is clear, and the polarization of the CO group is quite different in both cases. The proton is shielded much more efficiently in the HCO^+ case, as the Q^H value shows, even though it approaches the CO moiety toward the positively charged end. This already points toward covalency as an important factor in accounting for the stiffening phenomenon, more important for a HC interaction than for a HO one due to the smaller electronegativity difference between the atoms in the first case. Notice that the CO distance decreases from the isolated CO molecule in the HCO^+ case, but increases in the COH^+ one.

The origin of this very different behavior may be traced to the HC and HO delocalization indices in Table 7, which have a huge impact on δ^{CO}. The latter is much smaller in the COH^+ system, and this propagates the covalent energies, which are more stabilizing than those in the free CO molecule for the HCO^+ case and considerably less stabilizing in COH^+. Notice how, from all the data contained in the table, the behavior of $\Delta\delta^{CO}$ and ΔV_{xc}^{CO} stands out. As found before, δ's are very sensitive indicators of the CO behavior. The CO stiffening in HCO^+ is thus a covalent effect, which as our examples show, and in agreement with Lupinetti and co-workers,[23] is triggered by the particular polarization pattern generated by an RCO^+ arrangement, characterized by a smaller CO charge separation than in COR^+. We want to stress that, as found in other IQA studies,[36] bond lengths and probably force constants are strongly correlated to the V_{xc} component of the interaction energy. We can see that the CO electrostatic contribution is clearly more stabilizing in the COH^+ arrangement, and that even the total E_{int}^{CO} may exceed that found in HCO^+. However, the general d^{-1} distance dependence of V_{cl} makes this term vary more slowly than V_{xc}, which changes exponentially with the distance of

Table 8. Topological Charges and Sharing Indices for Several DFT Descriptions of the $[Ag(CO)_2]^+$ and $[Au(CO)_2]^+$ Systems, Together with HF Data, All of Them at the MP2 Geometry[a]

	B3LYP	BLYP	BLYP-LC	M06-l	M06	M06-HF	HF
Q^{Ag}	0.711	0.695	0.701	0.728	0.706	0.739	0.770
Q^{C}	1.189	1.147	1.176	1.187	1.208	1.237	1.338
Q^{O}	−1.044	−0.995	−1.027	−1.050	−1.060	−1.107	−1.223
δ^{AgC}	0.576	0.610	0.579	0.573	0.573	0.510	0.482
δ^{AgO}	0.063	0.074	0.059	0.069	0.060	0.046	0.042
δ^{CC}	0.013	0.017	0.011	0.013	0.012	0.006	0.005
δ^{CO}	1.795	1.840	1.815	1.782	1.769	1.748	1.599
Q^{Au}	0.624	0.622	0.612	0.650	0.638	0.596	0.652
Q^{C}	1.200	1.152	1.190	1.193	1.209	1.272	1.371
Q^{O}	−1.012	−0.962	−0.996	−1.017	−1.028	−1.070	−1.196
δ^{AuC}	0.948	0.979	0.941	0.953	0.942	0.880	0.849
δ^{AuO}	0.119	0.133	0.111	0.127	0.114	0.092	0.085
δ^{CC}	0.047	0.055	0.042	0.047	0.040	0.034	0.027
δ^{CO}	1.748	1.791	1.772	1.737	1.732	1.709	1.559

[a] All data in atomic units.

the two centers. Larger classical terms at the expense of covalent contributions, as found in this case, usually lead to larger bond lengths and smaller force constants. Similar polarizations are obtained if the H atom is substituted by a positive point charge.

A comment on the values of δ upon inclusion of electron correlation is needed. It is now known that electron correlation tends to localize electrons in atomic basins beyond the HF independent electron model, so the number of effective pairs of electrons participating in bonding decreases, sometimes dramatically.[35] In this work, for instance, free δ^{CO} changes from 1.51 (HF) to 1.38 (CASSCF) on including our limited amount of correlation. Simple density functional calculations provide a much larger value, about 1.7, as seen in the caption of Table 2. This is due to the pseudo-single-determinant structure of the KS description, and to the smaller CO bond length predicted at this level of theory. A definitive value for CO is lacking, but δ changes are well reproduced by any description, as we are seeing.

We have also performed a comparison of the IQA descriptions for these linear carbonyls when several levels of theory are employed, including the approximate DFT descriptions previously described. Table 8 contains a survey of topological charges and sharing indices for the $[Ag(CO)_2]^+$ and $[Au(CO)_2]^+$ systems at the DFT level, with several density functionals to be compared with the CASSCF data contained in Table 6. Notice that introducing HF exchange increases, in general, the topological net charge of C and O and approaches the CASSCF values, which include a very limited amount of correlation (compare with the HF column). Any functional provides noticeably larger delocalization indices than our CASSCF results, with δ^{CO} close to 1.8. A comment on this large value has already been made in this paper. The DFT data also confirm how electron correlation increases back-donation, as measured by δ^{MO}, in agreement with general knowledge.

7. Discussion and Conclusions

The results explored in the previous sections show that the IQA view provides a real space image of bonding in simple metal carbonyls that is compatible with existing knowledge. Overall, IQA interactions show several general features that deserve further comment.

Most, if not all, of the IQA quantities show a very clear dependence on the total net charge and coordination of the complexes examined. As far as the ML interaction is concerned, for instance, Tables 1−6 show that V_{cl}^{ML} is basically controlled by the stoichiometry. As we move from mono- to hexacoordinated complexes, there is a clear tendency for the ML classical interaction to progress from destabilizing to stabilizing values. For a given stoichiometry, it evolves toward increasing stabilization as the net charge of the complex passes from positive to negative values. These trends are a result of the expected increase that Q^M experiences as both the coordination index and the net charge of the complex grow. ML covalency, measured by V_{xc}^{ML}, is again dependent on both parameters, but here a more subtle balance takes place. On one hand, larger coordinations saturate the metal binding ability, so V_{xc}^{ML} per ML link tends to decrease on going from mono- to hexacoordinated molecules. On the other hand, extra electrons minimize this saturation tendency, so the largest ML covalent energies appear on the negatively charged tetrahedral carbonyls. As a result of this interplay, except in the octahedral compounds, the total E_{int}^{ML} is dominated by covalency, and its largest values (which are always stabilizing) again occur for negatively charged tetrahedral, pentacoordinated, and octahedral systems, where large π-back-bonding exists. Similarly, the smallest total ML interactions are found in some positively charged complexes.

The change in the local properties of the CO moiety upon bonding has played a dominant role in the chemistry of metal carbonyls. We have found almost a full match between traditional thinking and the IQA relaxation quantities for CO. Figure 1 shows the change in the CO interaction parameters upon bonding. There, it is clear that the total CO interaction becomes clearly destabilized upon formation of the complexes, except in the Ag and Au dicarbonyls, and that this effect is overwhelmingly dominated by the change suffered by the electrostatic component, ΔV_{cl}^{CO}, which may be obtained by subtracting the much smaller xc component of the lower diagram. Polarization of the CO charge density upon coordination (which includes a charge transfer component) becomes the dominant energetic effect in CO. This conclusion is not affected much by the inclusion of ΔE_{self} for the C and O atoms, which is almost always negative, so the total CO deformation is generally positive, with minima appearing when Q^M is smallest for each stoichiometry. The change in the CO covalency, shown in the lower diagram of Figure 1, has been discussed in a coordination-like manner in previous sections. Here, it serves us to show that it is the change in the CO covalency which correlates with the CO distance and stretching frequency. So, despite the large electrostatic contributions due to M↔L charge transfer and polarization, it is electron sharing, i.e., electronic effects, which determines the basic signature of ML bonding.

Finally, we will consider an interesting correlation shown by our data.[33,34,42] As already commented upon, the value of δ^{MO}, expected to include negligible σ contributions, has been proposed as a measure of the intensity of π-back-

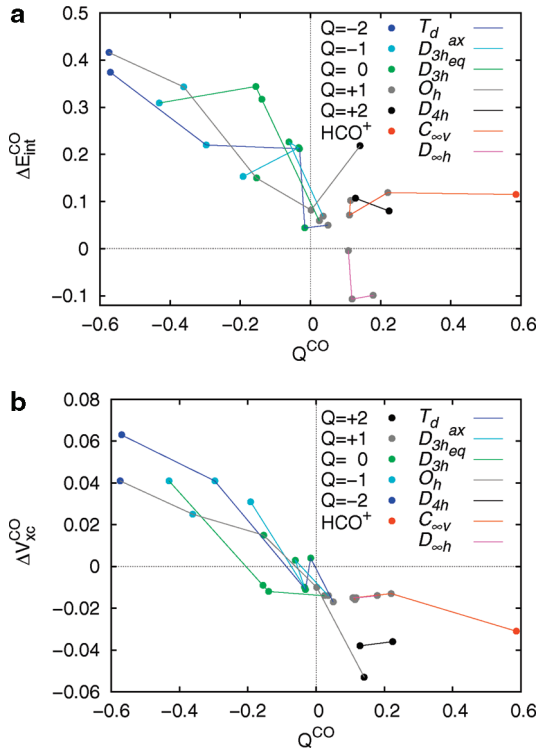

Figure 1. Comparison of the behavior of ΔV_{cl}^{CO} (upper diagram) and ΔV_{xc}^{CO} (lower diagram) versus the ligand topological charge (Q^{CO}) for the carbonyls examined in this work. Systems have been gathered by symmetry and stoichiometry, and a color code has been added to identify the total net charge of the complex.

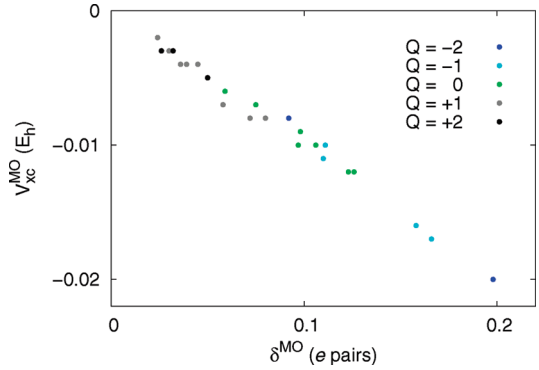

Figure 2. Correlation between V_{xc}^{MO} and δ^{MO} for the systems studied in this work. The total net charge of the complexes is indicated by the same color code used in Figure 1.

bonding in these systems.[5,25] We similarly expect that V_{xc}^{MO} will extract its energetic content. Figure 2 shows a nice linear correlation between these two quantities. The largest and smallest covalent energies and delocalization indices correspond to negatively and positively charged complexes, respectively. We must again stress that the small value of the energies involved, smaller than 15 kcal/mol, does not measure the energetic intensity of π-back-donation. It will always be the V_{xc}^{MC} component, mixed with σ donation, that dominates. Anyway, our data show that δ^{MO}, much easier to compute than V_{xc}^{MO}, may be used safely to measure π-back-donation. We will corroborate this in a forthcoming paper in which V_{xc}'s and δ's will be decomposed using DAFHs.

To conclude, we have applied the interacting quantum atoms approach (IQA) within the QTAIM to explore chemical bonding in real space in simple transition metal carbonyls. This is the first time that such an energetic viewpoint is provided for TM complexes, thanks to recent protocols devised to deal with effective core potentials in the IQA scheme.[43]

We have explored several classical and nonclassical compounds, with different stereochemistries, and at different levels of theory. As a general conclusion, the bonding image provided by our procedure does not change qualitatively with the inclusion of electron correlation, as noticed by other authors, and is consistent with previous knowledge. It however sheds light on some issues by providing an orbital invariant energetic description of the several metal−carbonyl interactions.

The topological charges of the metal have been found to be positive in all the systems examined, even in dianions. This is known, but clearly shows that formal oxidation states must be taken with care. As expected, π-back-donation in the standard DCD model accounts reasonably well for our findings, being cleanly related to the amount of electron sharing between the metal and the oxygen atom of each carbonyl group. Negative or neutral complexes show the traditional CO bond length elongation, accompanied by a decrease in both the CO bond order and the covalent energy of the CO bond. Interestingly, our analyses point toward nonnegligible multicenter character of the ML bonds, and several carbonyl groups may be involved in it when back-bonding is prominent, as revealed by unexpectedly large intercarbonyl CC delocalization indices. This issue needs to be further explored and will be the subject of further studies.

Covalency dominates the ML link and decreases on going from anions to cations for a given coordination and decreases as coordination increases. Simultaneously, the metal to ligand electrostatic interaction becomes more stabilizing on going from tetra- to hexacarbonyls, mimicking well-known solid state physics behaviors. V_{cl}^{ML}, although smaller than V_{xc}^{ML}, covers a rather full spectrum, from rather stabilizing (up to −120 kcal/mol) in negatively charged hexacarbonyls, passing through practically electroneutral in most tetrahedral compounds, to clearly destabilizing in some nonclassical systems. It is particularly interesting that the latter, which were originally thought to be mainly bonded by electrostatic forces, tend to be those systems which would not be stable without covalent contributions.

The IQA description of nonclassical carbonyls recovers many of the features already reported using other bonding analyses, showing that these features are rather robust, for instance, the larger covalency of the $[Ag(CO)_2]^+$ system with respect to the $Ag(CO)^+$ one and the reverse behavior of the gold cases. The stiffening of the CO bond is neatly revealed by larger covalent contributions for the CO interaction than those found in the isolated carbon monoxide molecule, even though the energetic changes derived from CO repolarization (as measuered by ΔV_{cl}^{CO}) are much larger. Stiffening is thus shown not to be a simple consequence of the electrostatic field imposed by the metal positive net charge, but of the complex reorganization of the CO moiety induced by it.

The energetic perspective provided by IQA may thus be added to the toolkit that the modern theory of chemical bonding in real space provides in transition metal chemistry. By adding interaction energy terms to other well tested indices, it may provide new insights into the field.

Acknowledgment. D.T. thanks the University of Milan and the Italian Ministry of Research (MIUR) for a Ph.D. grant that allowed his stay at Oviedo. M.A.B., E.F., and A.M.P. acknowledge financial support from the Spanish MICINN, Project Nos. CTQ2006-02976 and CTQ2009-08376, the European Union FEDER funds, the MALTA-Consolider program (CSD2007-00045), and the FICYT (IB09-019). P.M. thanks the Swiss National Science Foundation for support (project 200021_125313).

References

(1) Dewar, M. *Bull. Soc. Chim. Fr.* **1951**, *18*, C79.

(2) Chatt, J.; Duncanson, L. A. *J. Chem. Soc.* **1953**, 2929.

(3) Ziegler, T.; Rauk, A. *Inorg. Chem.* **1979**, *18*, 1755.

(4) Weinhold, F.; Landis, C. *Valency and Bonding. A Natural Bond Orbital Donor-Acceptor Perspective*; Cambridge Univ. Press: Cambridge, U. K., 2005.

(5) Macchi, P.; Sironi, A. *Coord. Chem. Rev.* **2003**, *238*−*239*, 383.

(6) Cortés-Guzmán, F.; Bader, R. F. W. *Coord. Chem. Rev.* **2005**, *105*, 3911.

(7) Pilme, J.; Silvi, B.; Alikhani, M. E. *J. Phys. Chem. A* **2003**, *107*, 4506.

(8) Matito, E.; Sola, M. *Coord. Chem. Rev.* **2009**, *253*, 647.

(9) Dapprich, S.; Frenking, F. *J. Phys. Chem.* **1995**, *99*, 9352.

(10) Davidson, E. R.; Kunze, K. L.; Machado, F. C. B.; Chakravorty, S. *Acc. Chem. Res.* **1993**, *26*, 628.

(11) Pyykkö, P. *Chem. Rev.* **1988**, *88*, 563.

(12) Johnson, J. B.; Klemperer, W. G. *J. Am. Chem. Soc.* **1977**, *99*, 713.

(13) D'Amico, K. L. D.; Trenary, M.; Shin, N. D.; Solmon, E. I.; McFeely, F. R. *J. Am. Chem. Soc.* **1982**, *104*, 5102.

(14) Cotton, F. A.; Wing, R. M. *Inorg. Chem.* **1965**, *4*, 314.

(15) Cotton, F. A. *Inorg. Chem.* **1963**, *3*, 702.

(16) Hall, M. B.; Fensk, R. F. *Inorg. Chem.* **1972**, *11*, 1619.

(17) Hurlbut, P. K.; Rack, J. J.; Luck, J. S.; Dec, S. F.; Webb, J. D.; Anderson, O. P.; Strauss, S. H. *J. Am. Chem. Soc.* **1994**, *116*, 10003.

(18) Souma, Y.; Sano, H. *J. Org. Chem.* **1973**, *38*, 3633.

(19) Bach, C.; Wilner, H. *Angew. Chem., Int. Ed.* **1996**, *108*, 2104.

(20) Sierraalta, A.; Frenking, G. *Theor. Chim. Acta* **1997**, *95*, 1.

(21) Szilagyi, R. K.; Frenking, F. *Organometallics* **1997**, *16*, 4807.

(22) Goldman, A. S.; Krogh-Jespersen, K. *J. Am. Chem. Soc.* **1996**, *118*, 12159.

(23) Lupinetti, A. J.; Fau, S.; Frenking, F.; Strauss, S. H. *J. Phys. Chem.* **1997**, *101*, 9551.

(24) Ehlers, A. W.; Dapprich, S.; Vyboishchikov, S. F.; Frenking, F. *Organometallics* **1996**, *15*, 105.

(25) Macchi, P.; Garlaschelli, L.; Sironi, A. *J. Am. Chem. Soc.* **2002**, *124*, 14173.

(26) Ponec, R.; Lendvay, G.; Chaves, J. *J. Comput. Chem.* **2008**, *29*, 1387.

(27) Ponec, R. *J. Math. Chem.* **1997**, *21*, 323.

(28) Ponec, R. *J. Math. Chem.* **1998**, *23*, 85.

(29) Scherer, W.; Eickerling, D.; Shorokhov, D.; Gullo, G. S.; McGrady, M.; Sirsch, P. *New J. Chem.* **2006**, *30*, 309.

(30) Martín Pendás, A.; Blanco, M. A.; Francisco, E. *J. Chem. Phys.* **2004**, *120*, 4581.

(31) Martín Pendás, A.; Francisco, E.; Blanco, M. A. *J. Comput. Chem.* **2004**, *26*, 344.

(32) Blanco, M. A.; Martín Pendás, A.; Francisco, E. *J. Chem. Theory Comput.* **2005**, *1*, 1096.

(33) Francisco, E.; Martín Pendás, A.; Blanco, M. A. *J. Chem. Theory Comput.* **2006**, *2*, 90.

(34) Martín Pendás, A.; Blanco, M. A.; Francisco, E. *J. Comput. Chem.* **2007**, *28*, 161.

(35) Martín Pendás, A.; Francisco, E.; Blanco, M. A. *J. Phys. Chem. A* **2006**, *110*, 12864.

(36) Martín Pendás, A.; Blanco, M. A.; Francisco, E. *J. Chem. Phys.* **2006**, *125*, 184112.

(37) Martín Pendás, A.; Blanco, M. A.; Francisco, E. *J. Comput. Chem.* **2009**, *30*, 98.

(38) Martín Pendás, A.; Francisco, E.; Blanco, M. A.; Gatti, C. *Chem.*−*Eur. J.* **2007**, *13*, 9362.

(39) Francisco, E.; Martín Pendás, A.; Blanco, M. A. *J. Chem. Phys.* **2007**, *126*, 094102.

(40) Martín Pendás, A.; Francisco, E.; Blanco, M. A. *J. Phys. Chem. A* **2007**, *111*, 1084.

(41) Martín Pendás, A.; Francisco, E.; Blanco, M. A. *J. Chem. Phys.* **2007**, *127*, 144103.

(42) Martín Pendás, A.; Francisco, E.; Blanco, M. A. *Phys. Chem. Chem. Phys.* **2007**, *9*, 1087.

(43) Tiana, D.; Francisco, E.; Blanco, M. A.; Martín Pendás, A. *J. Phys. Chem. A* **2009**, *113*, 7963.

(44) Bader, R. F. W. *Atoms in Molecules*; Oxford University Press: Oxford, U. K., 1990.

(45) McWeeny, R. *Methods of Molecular Quantum Mechanics*, 2nd ed.; Academic Press: London, 1992; Chapter 14.

(46) Sherwood, D. E.; Hall, M. B. *Inorg. Chem.* **1983**, *22*, 93.

(47) Barnes, A.; Ros, A.; Bauschlicher, C. W., Jr. *J. Chem. Phys.* **1990**, *93*, 609.

(48) Lupinetti, A. J.; Jonas, V.; Thiek, W.; Strauss, S. H.; Frenking, F. *Chem.*−*Eur. J.* **1999**, *5*, 2573.

(49) Schmidt, M. W.; Baldridge, K. K.; Boatz, J. A.; Elbert, S. T.; Gordon, M. S.; Jensen, J. H.; Koseki, S.; Matsunaga, N.; Nguyen, K. A.; Su, S. J.; Windus, T. L.; Dupuis, M.; Montgomery, J. A. *J. Comput. Chem.* **1993**, *14*, 1347.

(50) Hay, P. J.; Wadt, W. R. *J. Chem. Phys.* **1985**, *82*, 299.

(51) Wang, Y. G.; Werstiuk, N. H. *J. Comput. Chem.* **2003**, *24*, 379.

CT9006629